THE JOURNAL OF PHYSICAL CHEMISTRY B

Article

Visualization of Two-Dimensional Single Chain Conformations Solubilized in a Miscible Polymer Blend Monolayer by Atomic Force Microscopy

Kouki Sugihara, and Jiro Kumaki

J. Phys. Chem. B, **Just Accepted Manuscript** • DOI: 10.1021/jp303063c • Publication Date (Web): 08 May 2012

Visualization of Two-Dimensional Single Chain Conformations Solubilized in a Miscible Polymer Blend Monolayer by Atomic Force Microscopy

Kouki Sugihara,[1] *and Jiro Kumaki*[*]

Department of Polymer Science and Engineering, Graduate School of Science and Engineering, Yamagata University, Yonezawa, Yamagata 992-8510, Japan

RECEIVED DATE (to be automatically inserted after your manuscript is accepted if required according to the journal that you are submitting your paper to)

* To whom corresponding should be addressed. E-mail: kumaki@yz.yamagata-u.ac.jp

[1] Present: Yokohama Rubber Co., Ltd.

ABSTRACT

Polymer Langmuir monolayers spread on a water surface are one of the best models for two-dimensional (2D) polymer, and have been extensively studied. However, the most fundamental issue in understanding a 2D film – the polymer chain packing in the film - is still not well-understood, especially from the experimental point of view. Direct observation of the chain packing by microscopy at a molecular level, such as by atomic force microscopy (AFM), might be one of the most promising ways to study this issue, however, due to the limited resolution of the method, the chain packing of polymer cannot be resolved by AFM, except for especially large polymers. Here, we show that a mixed monolayer of vinyl polymers, poly(methyl methacrylate) (PMMA) and poly(*n*-nonyl acrylate) (PNA)

was miscible at a low surface pressure, and if a small amount of PMMA chains was solubilized in a PNA monolayer, the isolated PMMA chains in the PNA monolayer were, for the first time, successfully visualized by AFM with a clear contrast, which originated from a difference of rigidities of the polymers due to their different glass transition temperatures (105°C(PMMA), -89°C(PNA)). The PMMA chains were found to strongly interpenetrate into the PNA monolayer, with a radius of gyration ($R_{g(PMMA)}$) that was several times larger than that of the 2D ideal chain (segregated-chain). Furthermore, the radius scaled with the molecular weight of the PMMA (M_{PMMA}) as $R_{g(PMMA)} \propto M_{PMMA}^{0.63}$, which was between the scaling of the 2D ideal chain (segregated chain), $R_g \propto M^{0.5}$, and the 2D chain in good solvent, $R_g \propto M^{0.75}$. On the other hand, $R_{g(PMMA)}$ was independent of the molecular weight of the PNA matrix over a wide range. These results indicate that the PNA/PMMA monolayer is a strongly miscible system, although the $R_{g(PMMA)}$ scaling with M_{PMMA} (0.63) is somewhat smaller than that expected for a 2D chain in good solvent systems (0.75). The generation of molecular level information by direct observation of polymer chains in 2D blend films should improve our understanding of polymer 2D films.

Keywords: Langmuir-Blodgett film, poly(methyl methacrylate), poly(*n*-nonyl acrylate), interpenetration

1. Introduction

Polymer monolayers spread on a water surface are superior in mechanical and thermal stability in comparison with monolayers composed of small molecules, and thus, they have been extensively studied for possible applications as functional thin films.[1] Polymer monolayers are also an ideal model for the study of polymer chains in two-dimensional (2D) states and the structure and properties of such 2D states are also a subject of intense study. The 2D ideal chain is a 2D projection of a 3D ideal chain, and its radius of gyration, R_g, scales as $R_g \propto N^{0.5}$, similar to that of a 3D ideal chain.[2] de Gennes first suggested that since a 2D ideal chain could be built up to the 2D bulk density without interpenetrating into other chains, the polymer chains in a 2D film may exist as perfectly segregated chains.[2] Note that the compactness of the polymer does not necessarily imply disc-like shapes minimizing the perimeter of

the chain. A Monte Carlo simulation for a tangent hard disk model of 2D polymer indicated that the chain did not strongly segregate and considerable interpenetration between polymer chains was observed.[3] On the other hand, recent molecular dynamics simulations of a bead-spring model of self-avoiding chains in a 2D melt with chain lengths up to N=2048 showed that the chains adopted highly segregated conformations with irregular perimeters and patches of them gathered together to form 2D films.[4,5] The R_g of the chain scaled as $R_g \propto N^{0.5}$, similar to that of the 2D ideal chain, however, the chain statistics were completely different from those of the 2D Gaussian chain, thus, is not ideal. And the fractal perimeter of the chain was found to obey the contact exponent predicted by Duplantier.[6]

Experimental data on chain packing in a strict 2D state is still limited. Most previous experiments to evaluate chain expansion in thin polymer films were performed by scattering techniques,[7] therefore measurements on polymer chains in a strict 2D state that was only one monomer thick were difficult due to the extremely limited scattering volume of the 2D film. Thus, the alternative of observing 2D film by microscopy is more promising, and indeed a limited numbers of studies using microscopy have been reported. Maier and Rädler observed micrometer-long strands of fluorescence-labeled DNA adsorbed two-dimensionally on a cationic lipid membrane using fluorescent microscopy.[8,9] In a dilute state, the radius of gyration of the isolated DNA chains scaled with the number of base pair, N, as $R_g \propto N^{0.79}$, which was close to the scaling expected for a 2D self-avoiding chain, $R_g \propto N^{0.75}$.[2] In a condensed state, if a DNA mixed with DNAs of the same molecular weight, it adopted a compressed conformation, similar to that expected from de Gennes's segregated model. On the other hand, if the DNA mixed with lower molecular weight DNAs, it adopted an expanded conformation, consistent with the behavior commonly observed in 3D states.[10] However, quantitative results with a scaling value were not reported for the 2D condensed states in this case. Aoki and Ito observed fluorescence-labeled poly(methyl methacrylate) (PMMA) solubilized in an unlabeled PMMA monolayer by scanning near-field optical microscopy (SNOM), and showed that the polymer chains were highly segregated and found a value of R_g was in good agreement with that expected for a 2D ideal chain.[11] They also showed that poly(isobutyl methacrylate) (PiBMA) chains were respectively expanded or collapsed when dissolved

in a monolayer of a low, or similar, molecular-weight PiBMA,[12] behavior that is qualitatively consistent with that commonly observed in 3D states, but again quantitative scaling was not reported.

However, several reports have been contradicted the 2D segregated model. Wang and Foltz synthesized thick flexible polymer tubes with a large diameter of 20 nm by crosslinking a rod-like micelle of a block copolymer formed in a selected solvent, and observed 2D packing of the tubes on a substrate by AFM.[13] They showed that in a 2D dispersed state, the polymer tubes were collapsed and scaled as $R_g \propto L^{0.51}$, where L is the contour length of the tube. But, in a 2D condensed state, the tubes highly interpenetrated into other tubes with a scaling of $R_g \propto L^{0.625}$, in contradiction to the segregated model. As a polymer tube is much thicker than conventional polymer chains, it is still not clear whether the interpenetrated structure observed for the polymer tube is valid for monolayers of conventional polymers. We also successfully observed chain packing of a dense Langmuir monolayer of rigid-rod helical poly(phenyl isocyanide)s bearing long *n*-decyl chains as the pendant groups.[14] The polymer formed a helical rod structure with a chain-chain distance about 2.6 nm due to the long alkyl side chain spacer. The molecular packing in the Langmuir monolayer deposited on a substrate was successfully observed by AFM with clear images of whole chains. The chains were packed into the 2D film without any chain stacking, and were strongly interpenetrated with each other, again in contradiction to the 2D segregated model. However, the polymer was significantly rigid, with the persistence length of 220 nm, that we cannot deny that the strong interpenetration may partially originate from the rigidity of the polymers.

Direct observation of chain packing at a molecular level by AFM should be a most promising way to evaluate the structures in a film. However, observation of the molecular-level chain packing for conventional polymers is still challenging even by AFM because of the limited resolution of the method.[15]

On the other hand, polymer blend monolayers spread on a water surface also have been extensively studied.[16] The miscibility of polymer blends in monolayers was originally studied by the surface pressure-area (π–A) isotherms,[16a,b-h,n] then later with the aid of various methods, such as

ellipsometory,[16i] Brewster angle microscopy,[16o] fluorescence microscopy,[16m] transmission electron microscopy (TEM),[16k] scanning electron microscopy (SEM),[16g] and more recently AFM.[16j,k,m,17] However, no direct observation of chain packing in polymer blend monolayer has been achieved even by AFM. Recently, we studied a mixed Langmuir monolayer of PMMA and poly(*n*-nonyl acrylate) (PNA) by π–A isotherms and AFM, and found that the monolayer was thermodyanamically miscible at low surface pressures.[17] Since the rigidities of PMMA and PNA are very different due to their differing glass transition temperatures (105 ºC(PMMA), -89 ºC(PNA)),[18] we thought that if a small amount of PMMA chains are solubilized in a PNA monolayer, the rigid isolated PMMA chains may be resolved by AFM. As detailed later, we did successfully observed PMMA chains solubilized in a PNA monolayer, and were able to systematically evaluate the R_g of PMMA as a function of both the PMMA and matrix PNA molecular weights. To our best knowledge, this is the first observation of a polymer chain solubilized in a conventional polymer Langmuir monolayer. In the polymer blend system, the R_g of PMMA should be affected by the interaction between the component polymers as well as the 2D dimensionality. We believe detailed evaluation of chain packing in such monolayer at the molecular levels will improve our understanding of polymer 2D films.

2. Experimental Section

Materials. PMMAs with number average molecular weights (M_n) and molecular weight distribution (M_w/M_n), 2.10 × 10^5, 1.02 (PMMA(210k)); 7.42 × 10^5, 1.03 (PMMA(742k)), and 1.99 × 10^6, 1.08 (PMMA(1990k)), were purchased from Showa Denko (Tokyo, Japan). PMMAs with M_n = 1.26 × 10^5, M_w/M_n = 1.05 (PMMA(126k)), and 2.92 × 10^5, 1.02 (PMMA(292k)) were purchased from Polymer Laboratories Ltd. (Shropshire, UK). PNAs with M_n = 7.00 × 10^3, M_w/M_n = 1.30 (PNA(7k)); 1.30 × 10^4, 1.50 (PNA(13k)); 1.00 × 10^5, 1.16 (PNA(100k)), and 5.50 × 10^5, 1.19 (PNA(550k)) were purchased from Polymer Source (Montreal, Canada). Highly-purified benzene (Infinity Pure, Wako Chemicals, Osaka, Japan) was used as the solvent for the spreading solutions without further purification. Water was purified by a Milli-Q system and used as the subphase for the LB investigations.

***π–A* Isotherm Measurements and Langmuir-Blodgett (LB) Film Preparations for AFM.** The *π–A* isotherm measurements of a PMMA, PNA, and their mixtures were done as follows. Solutions of PMMA, PNA, and their mixture in benzene having a total polymer concentration from 6×10^{-5} to 1×10^{-4} g/mL were spread on a water surface at 23 ºC in a commercial LB trough with an area of 60 × 15 cm^2, and an effective moving barrier length of 15 cm (FSD-300AS, USI, Japan). The surface pressure was measured using filter paper as the Wilhelmy plate. The *π–A* isotherms were measured at a constant compression rate with a moving barrier speed of 0.5 mm/s. A monolayer was deposited onto a piece of freshly cleaved mica by pulling it out of the water at a rate of 4.2 mm/min, while compressing the monolayer at a constant pressure (the vertical dipping method).

In order to evaluate the reversibility of the chain conformation during hierarchical phase separation, a monolayer was deposited at constant surface pressures during a compression-expansion cycle, and observed by AFM. The compression and expansion rates for the reversibility investigation were 0.5 mm/s.

AFM Observations. After drying the deposited monolayers in vacuo, they were observed by a commercial AFM (NanoScope IIIa or IV/multimode AFM unit, Bruker AXS, Santa Barbara, CA, USA) with standard silicon cantilevers (PointProbe, NCH, NanoWorld, Neuchâtel, Switzerland) in air in the tapping mode. The typical settings of the AFM observations were as follows: a drive amplitude of 1.0–1.3 V, a set point of 0.65–1.20 V, and a scan rate from 1.80 to 3 Hz. The AFM images obtained are presented without any image processing except flattening. The radius of gyration of PMMA chains was evaluated by *ImageJ*, a public domain software from the National Institute of Health using the moment calculator plug-in by F. Richard, or by *2D Single Molecules*, freeware by Y. Roiter and S. Minko, available for download at http://people.clarkson.edu/~sminko. The radii of the gyration estimated by the both software packages were confirmed to be in good agreement.

3. Results and Discussion

3.1. *π–A* Isotherms and Phase Diagram of Monolayers of PMMA / PNA Mixtures. Figure 1A shows *π–A* isotherms of PMMA(292K), PNA(13K), and their mixtures (PMMA/PNA=90/10, 75/25,

50/50, 25/75, 10/90, and 1/100 by weight fraction). The π–A isotherms were similar to those reported previously for a PMMA(M_n=1.96 × 10^4, M_w/M_n=1.03) / PNA(13K) mixtures.[17] The PMMA monolayer (red line) showed a condensed-type π–A isotherm without any clear transition, and it collapsed around 50 mN/m. The PNA monolayer (black line) also showed a condensed-type π–A isotherm but it collapsed at a lower surface pressure around 20 mN/m, which resembled a plateau transition. On the other hand, PMMA/PNA mixtures showed clear plateau transitions. PMMA/PNA mixtures with the PMMA content higher than or equal to 50 weight %, PMMA/PNA = 50/50 (blue line) , 75/25 (orange) and 90/10 (green) had a single plateau transition around 15 mN/m, while a mixture with a PMMA content less than 50 weight %, PMMA/PNA = 25/75 (light green line) and 10/90 (gray), showed two plateau transitions at around 16 and 20 mN/m. The lowest weight fraction of PMMA, 1/100 (pink) showed only a small first transition at around 16 mN/m (see, magnified π–A isotherm in Figure 1B), with the steep increase of the surface pressure after the second plateau being undetectable due to the small PMMA content in these measurement conditions. In the previous report,[17] we identified these transitions as follows, based on the π–A isotherm results and the AFM observations of monolayers deposited on mica. At a low surface pressure, PMMA/PNA mixed monolayers are miscible and both the PMMA and PNA spread on the water surface. At the first transition around 15 mN/m, the monolayer hierarchical phase separates with the major component spread on the water surface as a monolayer, on top of which the minor component separated out. At the second transition which was observed only for PNA-rich mixtures (10/90, 25/75, and 1/100) at around 20 mN/m, the hierarchical phase separation with a lower monolayer of the major PNA and an upper layer of the minor PMMA component formed at the first transition, inverted relative to the previous phase. This phase inversion occurred, because at this surface pressure, the PNA monolayer was no longer stable, but the PMMA still formed a stable monolayer on the water surface. We confirmed the hierarchical phase separation was completely reversible depending on the surface pressure, indicating that these were true thermodynamical transitions.

Figure 2A shows a phase diagram of the hierarchical phase separation of the PMMA/PNA mixtures. The points were determined based on the first inflection points of the π–A isotherms of the blends. The surface pressure at the phase separation depended on the composition of the blends. Figure 2B is a schematic representation of the hierarchical phase separation of a PMMA/PNA mixture with an off-critical composition. At a low surface pressure, red polymer chains are solubilized in a monolayer of black polymer chains, but at a higher surface pressure, they separate out and aggregate on top of the monolayer of the black polymer chains. In this paper, we focus on compositions with a small amount of PMMA solubilized in a major PNA monolayer, thus the red and black chains correspond to PMMA and PNA in this study, respectively. At first we will discuss chain packing in the miscible region, and later show a hierarchical phase separation at higher surface pressure.

3.2. Visualization of PMMA Chains Solubilized in a PMMA/PNA Miscible Monolayer. Figure 3A shows AFM height images of monolayers of PMA(13k)/PMMA(1990k) =100/20, 100/10, and 100/1 wt/wt mixtures deposited on mica in a miscible region at a surface pressure of 1 mN/m. In this study, a monolayer for AFM observation was mainly deposited at a surface pressure as low as 1 mN/m, at a minimum surface pressure in order to obtain continuous monolayers while minimizing over compression of the monolayers. Thus, the monolayers observed here were closest to the 2D states. Chain-like structures which are about 0.3 nm higher than the matrix monolayer were diluted with a decrease in the PMMA contents in the mixtures. The number of the chain-like structures for the PNA/PMMA = 100/1 wt/wt mixture was 3 μm^{-2} on average, which was in good agreement with the number of the PMMA chains in the monolayer expected from the LB deposition conditions (N_{PMMA}(LB) = 3 μm^{-2}). These results indicate that the chain-like structures are actually PMMA chains solubilized in the PNA monolayer. To our best knowledge, this is the first example of visualization of polymer chains solubilized in a miscible blend monolayer of conventional polymers.

The rigidity of PMMA is very different from that of PNA due to the difference in their glass transition temperatures (T_g), which are 105 ºC for PMMA and -89 ºC for PNA.[18] Therefore, if both the polymers

are tapped at the room temperature by a cantilever with the same tapping force, the PMMA chains are detected as higher than the PNA monolayer. The PNA monolayer is more flexible than the PMMA, thus it may escape the tip when it taps the monolayer, and this may also reduce the apparent thickness of the PNA monolayer. These may be the origin of the contrast of the PMMA chains solubilized in the PNA monolayer. The height difference observed in AFM images depended on the scanning conditions, especially on the tapping force, which slightly varied from image to image for optimizing the scanning conditions for the images and, as the result, the heights of the PMMA chains slightly changed from image to image.

3.3. Radius of Gyration of Various-molecular-weight PMMAs Solubilized in PNA(13k) Monolayers. Figure 4A shows AFM height images of miscible monolayers of PNA(13k) with small amounts of a different-molecular-weight PMMA(126k, 210k, 292k, 742k, and 1990k) (100/1 wt/wt) deposited on mica at a surface pressure of 1 mN/m. The numbers of the PMMA chains estimated form the LB deposition conditions, N_{PMMA}(LB) and the numbers of the PMMA chains observed in the AFM images, N_{PMMA}(AFM) are indicated in each image, and they are in good agreement, indicating the chain-like structures are the PMMA chains. The size of the PMMA chains increased with the molecular weight of the PMMAs. Figure 4B summarized histograms of the radius of gyration of the PMMA chains determined from the AFM images. The radius of gyration of the PMMA chains increased with the molecular weights of the PMMAs.

Figure 5 shows a double–logarithmic plot of the root-mean-square radius of gyration, R_g, of PMMA chains in the miscible PNA(13k)/PMMA monolayers as a function of the molecular weight of the PMMA (red circles). The least square fitting line indicates a scaling of $R_g \propto M^{0.63}$. The blue line indicate scaling of the radius of gyration of 2D ideal chains, $R_g \propto M^{0.5}$, the absolute value of which was estimated by a 2D projection of radius of gyration of 3D ideal PMMA chains reported in the literatures.[19] The dotted line indicates the scaling for a 2D chain in a good solvent, $R_g \propto M^{0.75}$. The observed scaling, $R_g \propto M^{0.63}$, was between that of a 2D ideal chain and a 2D chain in good solvent. de Gennes pointed out that, as a single 2D ideal chain builds up a 2D bulk density without interpenetration

with other chains, the chains may strongly segregate from each other. The observed radius of gyration was about four to six times larger than that of the 2D ideal chain (segregated chain), indicating the PMMA chains expanded and extensively interpenetrated into the PNA chains. As shown in Figure 4, both chain ends were clearly recognizable, thus, these PMMA chains are not strongly segregated chains with irregular perimeters, but chains solubilized in the PNA monolayers. For reference, the green line in Figure 5 shows the radius of gyration of the PMMA chains estimated by assuming a PMMA chain forms a disk-like shape with an area equal to the limiting area, A_0, of PMMA π–A isotherms, which was determined by extrapolating the steepest slope of the π-A isotherm to zero surface pressure (0.99 m^2/mg). The area of the polymer is proportional to the molecular weight of PMMA, thus, R_g from A_0 scaled as $R_g \propto M^{0.5}$. PMMA formed a condensed-type π-A isotherm, and the PMMA chain adopts a condensed conformation. This rough estimation shows that the area of A_0 is comparable to those of the 2D ideal chains, and the PMMA chains solubilized in the PMMA/PNA monolayer extensively expanded and interpenetrated into the PNA monolayer.

As mentioned in the Introduction, the recent molecular dynamics simulations showed that chains in a 2D melt scales as $R_g \propto M^{0.5}$, similar to the 2D Gaussian (ideal) chains, but the chain statics were completely different from the Gaussian chains.[4,5] Thus, the chains in the 2D dense film may not be ideal. However, the R_g determined by AFM was compared to those of the 2D ideal chains in Figure 5, because not only the scaling with the molecular weight, but also the absolute values could be estimated as a 2D projection of the 3D ideal chains. As roughly compared to the R_g from A_0 of the π–A isotherms (green line in Figure 5), the compactness of the 2D chains in the monolayers should be comparable to those of the 2D ideal chains (blue line in Figure 5), thus the conclusion that the PMMA chains in the PMMA/PNA monolayers significantly expanded is basically valid.

The scaling of R_g of PMMA chains in the PNA/PMMA monolayer , $R_g \propto M^{0.63}$, was derived from the results using various molecular weight PMMAs solubilized in a single matrix monolayer of PNA(13k). So, if the R_g of PMMAs depended on the molecular weight of the PNA matrix, the scaling obtained here

may not correct. However, as shown below, the R_g of PMMA chains was independent of the molecular weight of PNA matrix, hence the scaling observed here is valid.

3.4. Radius of Gyration of PMMA(210k) Solubilized in PNA Monolayers with Various Molecular Weights. In Figure 6A, AFM height images of mixed monolayers of a different molecular weight PNA (7k, 100k, and 550k) with a small amount of PMMA(210k) (= 100/1 wt/wt) deposited on mica in the miscible region at 1 mN/m. As shown in Figure 6B and 6C, the radius of gyration of PMMA(210k) chains solubilized in PNAs with this wide range of molecular weights was unaffected by the molecular weight of the PNA matrixes. In a 2D homopolymer system, a polymer chain solubilized in a lower molecular weight polymer swells, while that solubilized in a larger molecular weight polymer should shrink; as mentioned, these behaviors were qualitatively confirmed by experiments for DNA[8,9] and PiBMA[12] monolayers. In the PNA/PMMA monolayer, the radius of gyration of the PMMA chain was not affected by the molecular weight of the PNA matrix, indicating that the PMMA chain is strongly solubilized in the PNA monolayer, although the scaling of R_g of PMMA with the molecular weight of the PMMA (0.63) was somewhat smaller than that expected for a 2D good solvent system (0.75).

3.5. Reversibility of Hierarchical Phase Separation of a PMMA Chain Solubilized in a PNA Monolayer as a Function of the Surface Pressure. Next, we will show that the R_g values observed here are close to those at the thermodynamically equilibrium states, and not determined kinetically. Figure 7A shows AFM height images of a monolayer of a PNA(13k)/PMMA(292k)=100/1 mixture deposited on mica during a compression-expansion cycle. The monolayer was first compressed to a surface pressure of 16 mN/m (1-4), then immediately expanded to 1 mN/m (4-6). The monolayers were miscible at lower surface pressures from 1 to 10 mN/m (1-3), the height differences of the PMMA chains from the PNA monolayers ranged from 0.31 nm to 0.52 nm, reasonably small values for chains solubilized in the monolayer, and the radius of gyration of the chains slightly decreased with compression as shown in Figure 7B. At 16 mN/m, near the inflection point of the π-A isotherm for the hierarchical phase separation shown in Figures 1B and 2A, the monolayer underwent a hierarchical phase separation with a PNA monolayer spread on the water surface as a monolayer, on top of which

the PMMA separated out and significantly aggregated (Figure 7A(4), see the inserted lower-magnification image (black frame)). The height of the aggregate from the PNA monolayer was 1.90 nm. The PMMA chains separated out on the PNA monolayer were not necessarily stable as a monolayer, because the hydrophilic groups were no longer anchored to the water surface, thus the PMMA formed a multilayer on the PNA monolayer. However, upon a subsequent expansion to 10 mN/m into the miscible regime, the PMMA chains were immediately solubilized into the monolayer again as shown in Figure 7A(5), and the chains slightly expanded with reducing the surface pressure (5-6). As shown in Figure 7B, the radius of gyration of the PMMA chains fully recovered after the compression-expansion cycle, indicating that the radius of gyration observed here was close to those at the thermodynamically equilibrium states under these experimental conditions. [20]

Finally, we will discuss a possible conformation change during the deposition of the monolayer from the water surface. We observed the PMMA/PNA monolayers after being deposited on mica in this study, thus, skeptical readers may suspect that the chain structures observed here might be different from those on the water surface. We do not deny the possibility of a small change in the observed structures, however, we believe this effect was small, as follows. First, the monolayers were deposited in a condensed state. If a monolayer is deposited in a dilute state, the chain may freely change the conformations, but in the condensed state, the polymer chain was surrounded by neighboring chains, thus, rearrangements of the chain conformations were expected to be suppressed. Second, mica is a hydrophilic substrate similar to the water surface. It adsorbs the ester groups of the PMMA and the PNA, in a manner similar to the water surface. In addition, there is an adsorbed water layer on the mica with a sub-nanometer thickness depending on the humidity of the surrounding air.[21] Third, as shown in this section, small conformational changes of the PMMA chains in the monolayer during a compression-expansion cycle were clearly observed after being deposited on the mica. If the conformations of the chains had significantly changed during the deposition, the small conformational changes observed here had not been recognized. Thus, if there were some conformational changes during the deposition process, it should be negligibly small in comparison to the conformational changes observed here.

4. Concluding Remarks

By using a miscible PMMA/PNA monolayer, isolated PMMA chains solubilized in the PNA monolayer were successfully observed by AFM, and their radius of gyration was quantitatively evaluated as a function of both the PMMA and matrix PNA molecular weights. Since chain packing in single-component monolayer of a conventional polymer is difficult to resolve by AFM, this appear to be the first observation of chain conformation in a conventional polymer monolayer by AFM.

The result showed the PMMA chains extensively expanded in the blend monolayer, and strongly interpenetrated into the PNA monolayer. The R_g of PMMA chains solubilized in PMMA/PNA monolayer scales as the molecular weight of the PMMA with a power of 0.63, that is, intermediate between the values of a 2D ideal chain (0.5) and that of a chain swollen in a good solvent (0.75). On the other hand, the R_g of PMMA(210k) chain solubilized in different molecular weight PNA matrices did not change, even for PNA molecular weights that varied from 1/30 to 2.6 times that of the PMMA(210k). Thus, although the R_g scaling with the PMMA molecular weight (0.63) was somewhat smaller than that expected for a 2D good solvent system (0.75), the constant R_g of a PMMA chain over a wide range of the molecular weight of PNA matrix indicates that the PMA/PMMA is a strongly miscible system.

PMMA formed a condensed-type π-A isotherms. The scaling analysis of π-A isotherms of polymers in a semidilute regime can be expressed as $\pi \approx C^{2\upsilon/(2\upsilon-1)}$, where C is the surface concentration, and υ is the power of R_g scaling with the molecular weight as $R_g \propto M^{\upsilon}$.[22,23] The value of υ has been estimated as 0.56[17] and 0.53[18], close to the value for a 2D ideal chain (0.5), thus, a PMMA chain spread on the water surface has a collapsed conformation. This collapse conformation was qualitatively confirmed by AFM observation of a PMMA monolayer deposited on mica in a dilute state.[24,25] Therefore, while a PMMA chain on the water surface adopts a collapsed conformation close to that of an 2D ideal chain, upon solubilization into a PNA monolayer, the conformation expanded and the υ value increased to 0.63.

The scaling, $R_{g(PMMA)} \propto M_{PMMA}^{0.63}$ was smaller than that expected for the 2D swollen chain in good solvents, $R_g \propto M^{0.75}$. At present, the reason for this deviation is not clear, but several possible reasons are described as follows. The first is a finite miscibility between PMMA and PNA, which may result in a reduction of $R_{g(PMMA)}$, especially for less miscible higher-molecular-weight PMMAs. As a result, the apparent scaling may become smaller. The second is a pseudo-two-dimensionality of polymer monolayers on the water surface. The theories and simulations deal with strictly 2D systems. Although a polymer monolayer is one of the best models available for 2D polymer systems, but it still has a finite thickness, small loops and trains may exist in the molecular scale. This may differentiate the scaling from a strictly 2D states.[26] The third is a strong interaction between the monolayer and the subphase, which is sometimes ignored in the ideal 2D systems that theories and simulations deal with. The conformation of PMMA chains observed in this work should be analyzed based on various interactions such as PMMA-PNA, PMMA-PMMA, PMMA-water, and PMMA-air interactions. Especially in the real 2D state, contribution of the polymer-subphase interaction should be dominant in order to keep the monolayer in the 2D state, which, however, is sometimes omitted in ideal 2D states used in theories and simulations. In addition to an experimental approach shown here, theoretical and simulational works are necessary to understand the real 2D state. We are currently investigating various miscible polymer blend systems, and the dependence of the scaling, υ, on the molecular weight of the dispersed and matrix polymers is being evaluated. We believe that the direct observation of polymer chains in monolayer as presented here will improve our understanding of 2D polymer systems.

Acknowledgment. This work was supported by a Grant-in-Aid for Scientific Research on Innovative Areas "Molecular Soft-Interface Science" (20106009), Scientific Research (B) (21350059, 23360108, 24350113), and Challenging Exploratory Research (23655208, 24655091) from the Ministry of Education, Culture, Sports, Science, and Technology, Japan.

References

(1) (a) Crisp, D. J. *J. Colloid Interface Sci.* **1946**, *1*, 49-70. (b) Gaines, G. L., Jr. *Insoluble Monolayers at Liquid-Gas Interfaces*; Interscience: New York, 1966. (c) Ulman, A. *An*

Introduction to Ultrathin Organic Films: From Langmuir-Blodgett to Self-Assembly; Academic Press: New York, 1991.

(2) de Gennes, P.-G. *Scaling Concepts in Polymer Physics*; Cornell University Press: London, 1979.

(3) Yethiraj, A. *Macromolecules* **2003**, *36*, 5854-5862.

(4) Mayer, H.; Kreer, T.; Aichele, M.; Cavallo, A.; Johner, A.; Baschnagel, J.; Wittmer, J. P. *Phys. Rev.* **2009**, *E*79, 050802-1-4.

(5) Mayer, H.; Wittmer, J. P.; Kreer, T.; Johner, A.; Baschnagel, J. *J. Chem. Phys.* **2010**, *132*, 184904-1-12.

(6) Duplantier, B. *J. Stat. Phys.* **1989**, *54*, 581-680.

(7) (a) Shuto, K.; Oishi, Y.; Kajiyama, T.; Han, C. C. *Macromolecules* **1993**, *26*, 6589-6594. (b) Brûlet, A.; Boué, F.; Menelle, A.; Cotton, J. P. *Macromolecules* **2000**, *33*, 997-1001. (c) Jones, R. L.; Kumar, S. K.; Ho, D. L.; Briber, R. M.; Russell, T. P. *Nature* **1999**, *400*, 146-149. (d) Jones, R. L.; Kumar, S. K.; Ho, D. L.; Briber, R. M.; Russell, T. P. *Macromolecules* **2001**, *34*, 559-567. (e) Ho, D. L.; Briber, R. M.; Jones, R. L.; Kumar, S. K.; Russell, T. P. *Macromolecules* **1998**, *31*, 9247-9252.

(8) Maier, B.; Rädler, O. *Phys. Rev. Lett.* **1999**, *82*, 1911-1914.

(9) Maier, B.; Rädler, O. *Macromolecules* **2000**, *33*, 7185-7194.

(10) Kirste, R. G.; Lehnen, B. R. *Makromol. Chem.* **1976**, *177*, 1137-1143.

(11) Aoki, H.; Morita, S.; Sekine, R.; Ito, S. *Polym. J.* (Tokyo) **2008**, *40*, 274-280.

(12) Aoki, H.; Anryu, M.; Ito, S. *Polymer* **2005**, *46*, 5896-5902.

(13) Wang, X.; Folts, V. J. *J. Chem. Phys.* **2004**, *121*, 8158-8162.

(14) Kumaki, J.; Kajitani, T.; Nagai, K.; Okoshi, K.; Yashima, E. *J. Am. Chem. Soc.* **2010**, *132*, 5604-5606.

(15) Recently, by use of 2D polymer monolayers deposited on substrates by Langmuir-Blodgett technique or solvent cast, polymer chain images with a resolution close to or slightly better than 1 nm were attained by AFM. For examples, see the following references. However, observation of polymer chain packing in 2D dense monolayers for conventional polymers is still beyond the resolution of AFM. (a) Kumaki, J.; Kawauchi, T.; Yashima, E. *J. Am. Chem. Soc.* **2005**, *127*, 5788-5789. (b) Kumaki, J.; Kawauchi, T.; Okoshi, K.; Kusanagi, H.; Yashima, E. *Angew. Chem., Int. Ed.* **2007**, *46*, 5348-5351. (c) Kumaki, J.; Kawauchi, T.; Ute, K.; Kitayama, T.; Yashima, E. *J. Am. Chem. Soc.* **2008**, *130*, 6373-6380. (d) Sakurai, S.-i.; Okoshi, K.; Kumaki, J.; Yashima, E. *Angew. Chem. Int. Ed.* **2006**, *45*, 1245-1248. (e) Sakurai, S.-i.; Okoshi, K.; Kumaki, J.; Yashima, E. *J. Am. Chem. Soc.* **2006**, *128*, 5650-5651. (f) Sakurai, S.-i.; Ohsawa, S.; Nagai, K.; Okoshi, K.; Kumaki, J.; Yashima, E. *Angew. Chem. Int. Ed.* **2007**, *46*, 7605-7608. (g) Kajitani, T.; Okoshi, K.; Sakurai, S.-i.; Kumaki, J.; Yashima, E. *J. Am. Chem. Soc.* **2006**, *128*, 708-709. (h) Onouchi, H.; Okoshi, K.; Kajitani, T.; Sakurai, S.-i.; Nagai, K.; Kumaki, J.; Onitsuka, K.; Yashima, E. *J. Am. Chem. Soc.* **2008**, *130*, 229-236. (i) Maeda, T.; Furusho, Y.; Sakurai, S.-i.; Kumaki, J.; Okoshi, K.; Yashima, E. *J. Am. Chem. Soc.* **2008**, *130*, 7938-7945. (j) Ohsawa, S.; Sakurai, S.-i.; Nagai, K.; Banno, M; Maeda, K.; Kumaki, J.; Yashima, E. *J. Am. Chem. Soc.* **2011**, *133*, 108-114. (k) For review, see. Kumaki, J.; Sakurai, S.-i.; Yashima, E. *Chem. Soc. Rev.* **2009**, *38*,737-746.

(16) (a) Wu, S.; Huntsberger, J. R. *J. Colloid Interface Sci.* **1969**, *29*, 138-147. (b) Gabrielli, G.; Puggelli, M.; Faccioli, R. *J. Colloid Interface Sci.* **1971**, *37*, 213-218. (c) Gabrielli, G.; Puggelli, M.; Faccioli, R. *J. Colloid Interface Sci.* **1973**, *44*, 177-180. (d) Gabrielli, G.; Puggelli, M.; Ferroni, E. *J. Colloid Interface Sci.* **1974**, *47*, 145-154. (e) Gabrielli, G.; Baglioni, P. *J. Colloid Interface Sci.* **1980**, *73*, 582-587. (f) Gabrielli, G.; Puggelli, M.; Baglioni, P. *J. Colloid Interface Sci.* **1982**, *86*, 485-500. (g) Caminati, G; Gabrielli, G.; Puggelli, M.; Farroni, E. *Colloid Polym.*

Sci. **1989**, *267*, 237-245. (h) Kawaguchi, M.; Nishida, R. *Langmuir* **1990**, *6*, 492-496. (i) Kawaguchi, M.; Nagata, K. *Langmuir* **1991**, *7*, 1478-1482. (j) Kawaguchi, M.; Suzuki, S.; Imae, T.; Kato, T. *Langmuir* **1997**, *13*, 3794-3799. (k) Yamamoto, S.; Tsujii, Y.; Fukuda, T. *Polymer* **2001**, *42*, 2007-2013. (l) Kawaguchi, M.; Suzuki, M. *J. Colloid Interface Sci.* **2005**, *288*, 548-552. (m) Ohkita, M.; Higuchi, M.; Kawaguchi, M. *J. Colloid Interface Sci.* **2005**, *292*, 300-303. (n) Lee, Y.-L.; Hsu, W.-P.; Lio, S.-H. *Colloids Surface A* **2006**, *272*, 37-47. (o) Li, B.; Marand, H.; Esker, A. R. *J. Polym. Sci. Part B: Polym. Phys.* **2007**, *45*, 3200-3318.

(17) Sasaki, Y.; Aiba, N.; Kumaki, J. *Macromolecules* **2010**, *43*, 9077-9086.

(18) Brandrup, J.; Immergut, E. H. ; Grulke, E. A. ed. *Polymer Handbook*, 4th ed.; Wiley-Interscience Publication.: New Jersey, 1999.

(19) Kurata, M.; Stockmayer, W. H. *Fortschr. Hoch polym. Forsch.* **1963**, *3*, 196.

(20) The thickness of PMMA hierarchically deposited on the PNA monolayer upon compression was still only 1.9 nm (Figure 7(4)). The T_g of this thin film of the PMMA may be significantly reduced from that of the bulk. Further if the PMMA thin film is spread on a water surface by the subsequent expansion of the monolayer, water should plasticize the film and further reduce the T_g of the PMMA. Therefore, the recovery of the once hierarchically phase-separated film into the miscible monolayer may not be surprising.

(21) Beaglehole, D.; Radlinska, E. Z.; Ninham, B. W.; Christenson, H. K. *Phys. Rev. Lett.* **1991**, *66*, 2084.

(22) Vilanove, R.; Rondelez, F. *Phys. Rev. Lett.* **1980**, *45*, 1502-1505.

(23) Vilanove, R.; Poupinet, D.; Rondelez, F. *Macromolecules* **1988**, *21*, 2880-2887.

(24) Kumaki, J.; Nishikawa, Y.; Hashimoto, T. *J. Am. Chem. Soc.* **1996**, *118*, 3321-3322.

(25) Kumaki, J.; Hashimoto, T. *J. Am. Chem. Soc.* **2003**, *125*, 4907-4917.

(26) Semenov, A. N.; Johner, A. *Eur. Phys. J. E* **2003**, *12*, 469-480.

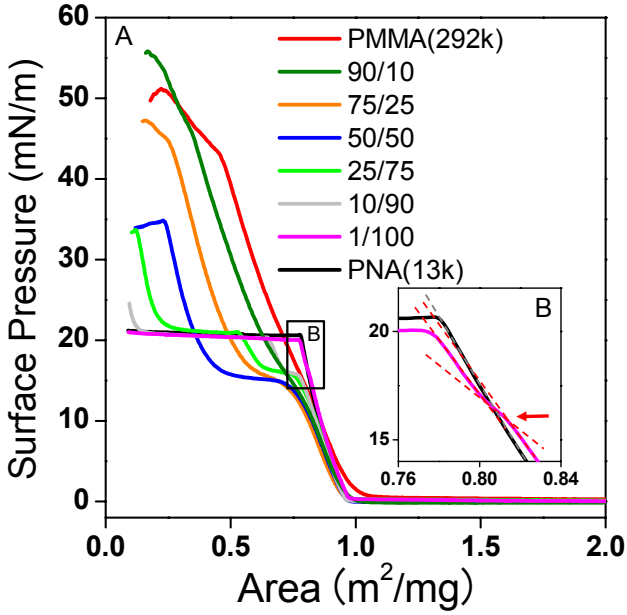

Figure 1. (A) π–A isotherms of monolayers of PMMA(292k), PNA(13k), and their mixtures (PMMA/PNA=90/10, 75/25, 50/50. 25/75, 10/90, and 1/100 wt/wt) on water. (B) Magnified π–A isotherms of monolayers of PNA (black) and PMMA/PNA=1/100 (pink) at the region indicated by the square (B) in (A).

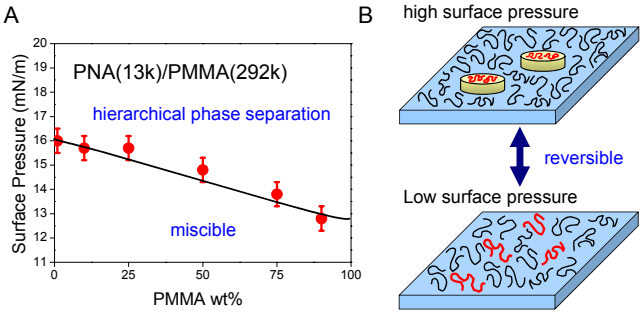

Figure 2. (A) Phase diagram of the hierarchical phase separation of the PMMA(292k) / PNA (13k) mixtures. The points were determined based on the first inflection points of the π–A isotherms for the corresponding compositions. (B) Schematic representation of the hierarchical phase separation of monolayers of PMMA and PNA mixtures with an off-critical composition.

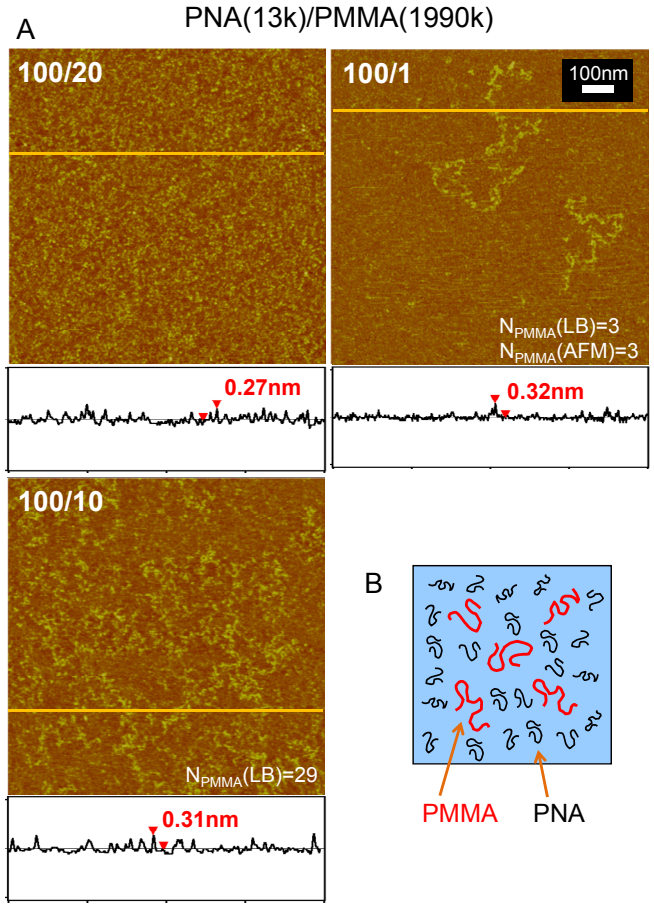

Figure 3. (A) Tapping-mode AFM height images of the monolayers of PNA(13k) / PMMA(1990k) mixtures (100/20, 100/10, and 100/1 wt/wt) deposited on mica in a miscible region at a surface pressure of 1 mN/m. The numbers of the PMMA chains estimated from the LB deposition conditions, N_{PMMA}(LB) (μm^{-2}) and observed in the AFM images as bright (higher) chains, N_{PMMA}(AFM) (μm^{-2}) were in good agreement as indicated in the image of the PNA/PMMA = 100/1 mixture. Height profiles along the yellow lines in the images are also shown. (B) Schematic representations of a PNA /PMMA miscible monolayer.

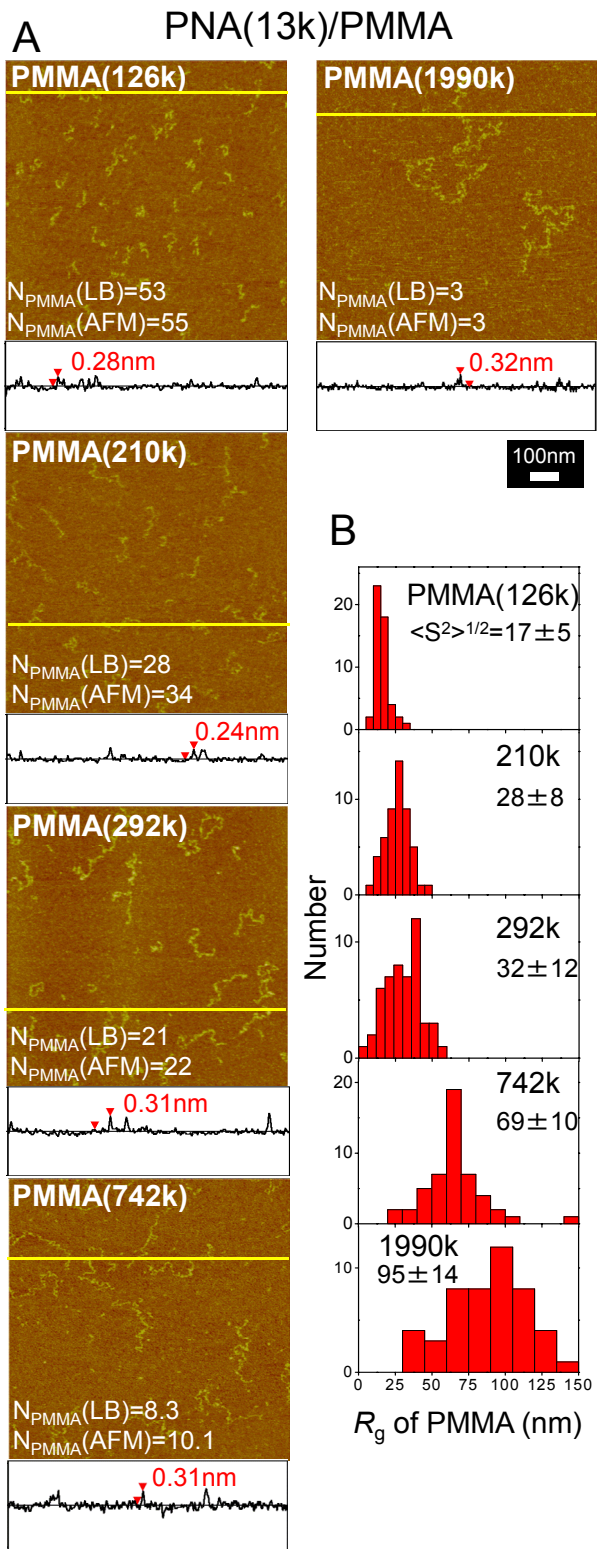

Figure 4. (A) Tapping-mode AFM height images of miscible monolayers of PNA(13k) / PMMA (126k, 210k 292k, 742k, and 1990k) mixtures deposited on mica at a surface pressure of 1 mN/m. The composition was PNA /PMMA = 100/1 wt/wt. The numbers of the PMMA chains estimated from the

LB deposition conditions, N_{PMMA}(LB) (μm^{-2}) and those observed in the AFM images as bright (higher) chains, N_{PMMA}(AFM) (μm^{-2}) were in good agreement as indicated in the images. Height profiles along the yellow lines in the images are also shown. Z-range of the images was 1.5 nm. (B) Histogram of the radius of gyration of the PMMA chains. The root-mean-square radius of gyration, $<S^2>^{1/2}$, is also indicated.

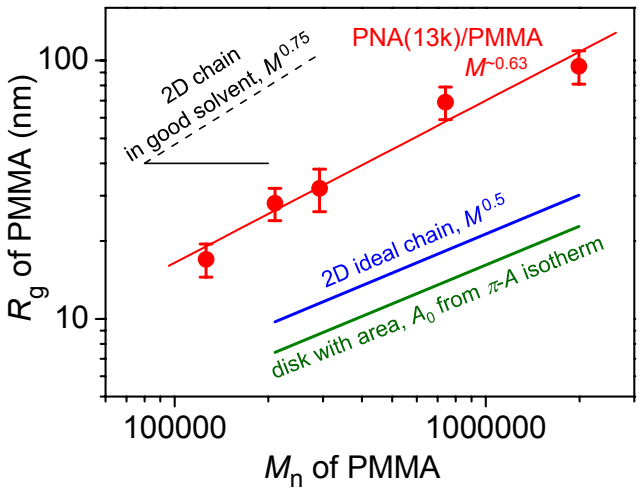

Figure 5. Double-logarithmic plot of the root-mean-square radius of gyration, R_g, of PMMA chains in miscible PNA(13k) / PMMA monolayers vs. the molecular weight of the PMMA (red circles). The red fit line indicates a scaling of $R_g \propto M^{0.63}$. The blue line indicates the scaling of 2D ideal chains, $R_g \propto M^{0.5}$, estimated by a 2D projection of the radius of gyration of a 3D ideal chain reported in reference 19. The dotted line indicates the scaling of a 2D chain in a good solvent, $R_g \propto M^{0.75}$. The green line indicates the radius of gyration of PMMA chains assumed to form a disk-like shape with an area given by the limiting area, A_0 of PMMA π-A isotherms.

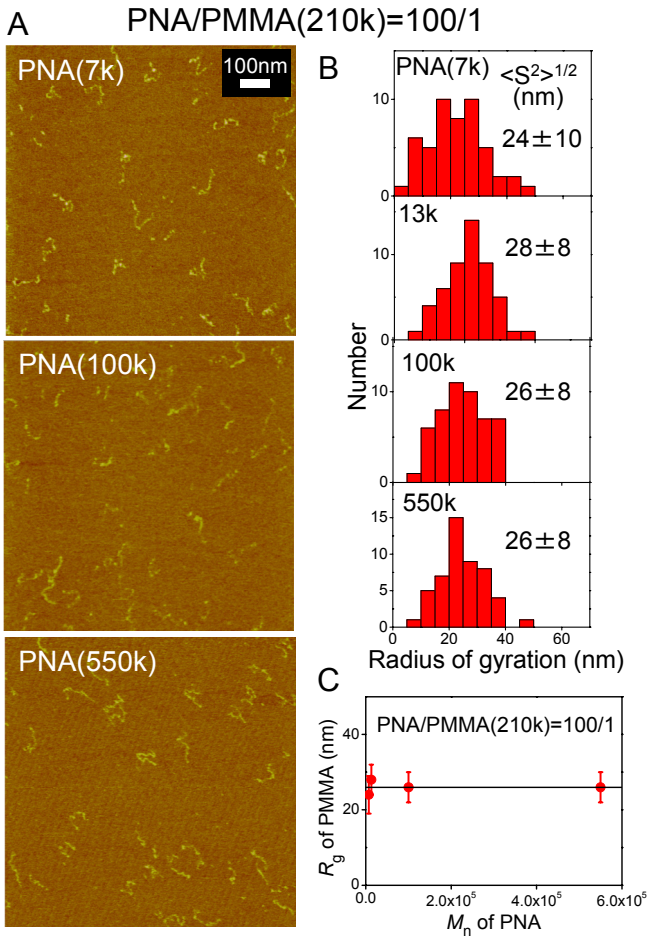

Figure 6. (A) Tapping-mode AFM height images of miscible monolayers of PNA(7k, 100k, and 550k) / PMMA (210k) mixtures deposited on mica at a surface pressure of 1 mN/m. The compositions were PNA /PMMA = 100/1 wt/wt. Z-range of the images was 1.5 nm. (B) Histogram of the radius of gyration of the PMMA chains in the miscible monolayers. The root-mean-square radius of gyration, $\langle S^2 \rangle^{1/2}$, is also indicated. (C) The root-mean-square radius of gyration of the PMMA as a function of the number-average molecular weight of the PNA.

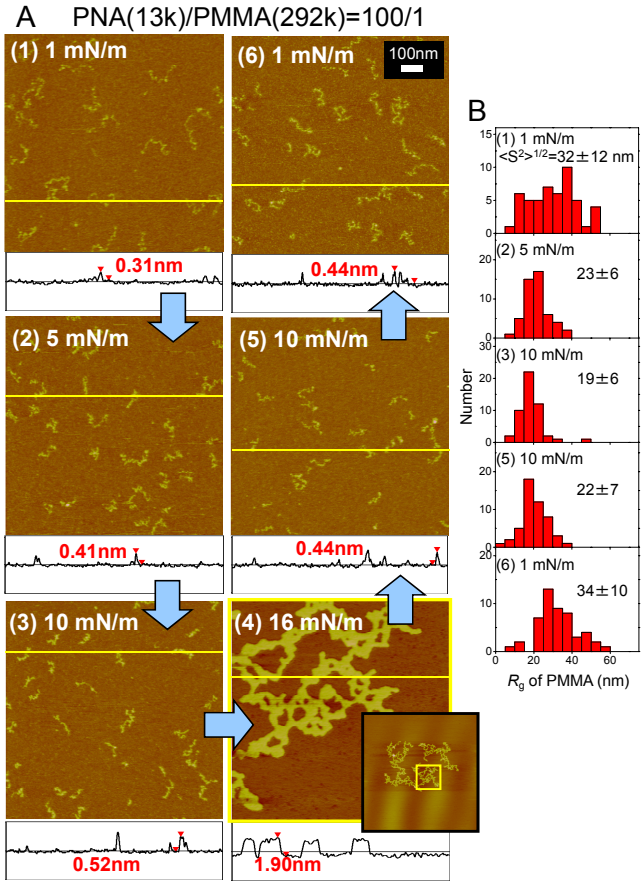

Figure 7. (A) Tapping-mode AFM height images of the monolayer of a PNA(13k) / PMMA(292k) mixture (100/1 wt/wt) deposited on mica during a compression–expansion cycle. The monolayer was first compressed to 16 mN/m (1-4), then, immediately expanded to 1 mN/m (4-6). The monolayer was miscible during (1)-(3), but at 16 mN/m it phase separated with a PNA monolayer spread on the water surface as a monolayer, on top of which the PMMA separated out and aggregated (4). The monolayer recovered its miscibility at the subsequent expansion (5-6). (B) Histogram of the radius of gyration of the PMMA chain during the compression-expansion cycle. The root-mean-square radius of gyration, $\langle S^2 \rangle^{1/2}$, is also indicated.

Table of Contents Graphic